Desalination and Water Treatment
www.deswater.com

doi: 10.5004/dwt.2018.21756

101 (2018) 193–202
January

Facile in situ synthesis and characterization of Ag_3PO_4 supported TiO_2 nanocomposite for visible light photocatalysis

Jamshaid Rashid[a,b], M.A. Barakat[b,c,*]

[a]*Department of Environmental Science, Faculty of Biological Sciences, Quaid-i-Azam, University, Islamabad 45320, Pakistan*
[b]*Department of Environmental Sciences, Faculty of Meteorology, Environment and Arid Land Agriculture, King Abdulaziz University, Jeddah 21589, Saudi Arabia, Tel. +966 02 6400000/64821; Fax: +966 02 6952364; emails: mabarakat@gmail.com (M.A. Barakat), jrashid@qau.edu.pk (J. Rashid)*
[c]*Central Metallurgical R&D Institute, Helwan 11421, Cairo, Egypt*

Received 30 April 2017; Accepted 5 December 2017

ABSTRACT

Facile in situ synthesis and characterization of stable Ag_3PO_4/TiO_2 nanoparticles for visible light photocatalytic water treatment has been reported. The surface morphology, crystal structure and chemical properties of the photocatalyst were characterized by using UV–Vis–NIR spectroscopy, field emission scanning electron microscopy, X-ray diffraction, X-ray photoelectron spectroscopy, transmission electron microscopy and nitrogen physisorption. The synthesized powder nanoparticles were polycrystalline in nature with calculated energy band gap in the range of 2.3–2.5 eV. Deposition of Ag_3PO_4 over the surface of TiO_2 resulted in increased stability of the photocatalyst and a significant shift in the UV absorption spectrum toward visible region. The photocatalytic experiments were performed in a batch reactor under 112 W cool white visible light irradiation with $\lambda > 400$ nm. The degradation of 2-chlorophenol (2-CP) as a model pollutant was investigated and reaction parameters for best catalyst performance were optimized. The catalyst showed complete degradation of 15 $mg{\cdot}L^{-1}$ 2-CP within 120 min while 92.5% degradation of 25 $mg{\cdot}L^{-1}$ 2-CP was achieved within 180 min under optimized conditions (i.e., 1 $g{\cdot}L^{-1}$ catalyst dose, at solution pH 3 and irradiation time of 180 min). The experimental results showed that the photocatalytic degradation results followed pseudo-first-order reaction kinetics and confirmed that Ag_3PO_4/TiO_2 has high potential for degradation of 2-CP from wastewater under visible light irradiation.

Keywords: Ag_3PO_4/TiO_2 nanoparticles; Advanced oxidation; 2-Chlorophenol; Visible light photocatalysis; Wastewater

1. Introduction

Recently, application of heterogeneous photocatalysis as an advance oxidation process has been seen as a potent solution for eradication of toxic organics from wastewater [1,2]. TiO_2 has become the most extensively studied photocatalyst since its use by Fujishima and Honda [3] for water splitting. However, the large energy band gap of TiO_2 (i.e., 3.2 eV) limits its use only to ultraviolet (UV) light driven photocatalysis which comprises only about 4% of solar spectrum incident on earth [4–8]. Current research focuses on the development of modified photocatalysts able to harness the visible spectrum of light which comprises the larger portion (~46%) of sunlight [9–11]. The strategies adopted to achieve such goal for instance may include creation of low energy impurity states within the TiO_2 band gap through noble metal doping or co-deposition that may promote electron hole pairs formation [12–15].

Ag_3PO_4 has been reported to effectively utilize visible light for water splitting and organic contaminants degradation [16–19]. A few studies suggest that Ag_3PO_4 shows up to

* Corresponding author.

12 times faster degradation of certain dyes compared with commercially available $TiO_{2-x}N_x$ and $BiVO_4$ with up to 90% quantum efficiency upon exposure to light with wavelength over 420 nm [19,20]. However, the instability and photocorrosion of Ag_3PO_4 in aqueous medium have been associated with the loss in photocatalytic efficiency over time, making catalyst recycling and reuse difficult [21,22]. It is therefore highly desirable to synthesize modified and stable photocatalysts that can effectively utilize the visible light harnessing power of Ag_3PO_4 nanoparticles with minimal consumption of expensive Ag precursors. Recently, a facile in situ preparation route for Ag_3PO_4 nanoparticles deposition onto the TiO_2 (Degussa P25) surface has been reported to increase both the stability and photocatalytic activity of TiO_2-based photocatalysts [23]. The current study comprises of in situ synthesis, characterization and evaluation of photocatalytic activity of stable and highly visible light active Ag_3PO_4/TiO_2 nanocomposite. The visible light photoactivity of the synthesized nanoparticles has been evaluated through degradation of 2-chlorophenol (2-CP) as a model organic pollutant. The choice of 2-CP was made due to the fact that phenol and its derivatives are commonly encountered organic pollutants in petrochemical, pharmaceutical and chemical industry wastewater causing severe environmental problems [24]. 2-CP is included in the priority pollutants list of United States Environmental Protection Agency (USEPA) and the European Union Water Framework Directive list of priority substances [25,26]. Also, the biological, physical and physicochemical water treatments are often ineffective or environmentally incompatible for degradation of such organic contaminants [27]. To best of our knowledge this is the first successful attempt to degrade 2-CP in visible light using an Ag_3PO_4/TiO_2 nanocomposite. The photocatalytic degradation pathways as a linear function of the concentrations of chlorophenol and catalyst have been considered for the interpretation of the kinetic data in this work.

2. Experimental

2.1. Materials

Silver nitrate, Degussa Titania (P25), and sodium phosphate (Sigma-Aldrich, USA) were used for catalyst preparation while 2-chlorophenol (2-CP) procured from Merck, USA, standard grade was utilized as pollutant. Deionized water was used for solution preparation. All other chemicals were also analytical grade.

2.2. Synthesis of Ag_3PO_4/TiO_2 photocatalyst

Synthesis of 0.3 M silver phosphate doped onto Degussa Titania (P25) was carried out using the in situ precipitation method reported by Zhang et al. [23]. Degussa P25 (0.02 mol) was dispersed in 50 mL distilled water and the solution was sonicated for 5 min. Silver nitrate (0.018 mol) was then added to the sonicated P25 solution and the resulting solution magnetically stirred for 10 min at 250 rpm. Sodium phosphate (0.006 mol) was dispersed in 50 mL distilled water and was then added dropwise to the previously prepared solution. The final solution was then magnetically stirred at 250 rpm for 5 h. A color change was observed from white to yellow. The resulting solution was then filtered, washed and dried in air overnight.

2.3. Material characterization

Characterization of the synthesized Ag_3PO_4/TiO_2 was performed by powder X-ray diffraction (XRD) measured with a Philips PANalytical Xpert PRO X-ray diffractometer using Cu Kα radiation under 45 kV accelerating voltage and 20 mA applied current. The surface area was determined by Quantachrome Autosorb IQ. After degassing the sample at a temperature of 200°C for 180 min, nitrogen porosimetry was performed at a temperature of 77 K over the 0 to 1 pressure ratio. X-ray photoelectron spectroscopic (XPS) surface analysis was performed using PHI 5000 VersaProbe II. Transmission electron microscopy (TEM) was performed on a Morgagni Transmission Electron Microscope and the images were obtained at an accelerating voltage of 60 kV. Field emission scanning electron microscopy (FESEM) was done by JSM-7500 F; JEOL, Japan, using parallel beam geometry and a multi-purpose thin film attachment. The optical reflectance of the synthesized powder material was recorded by PerkinElmer UV/Vis/NIR, Lambda 750 UV–Vis–NIR spectrophotometer equipped with integrating sphere, to record the diffuse reflectance spectra of the synthesized powder nanocomposite in the wavelength range of 200–900 nm. Kubelka–Munk (K–M) transformation was applied on the % R values to calculate the band gap of the synthesized Ag_3PO_4/TiO_2 by plotting $(F(R) \times h\upsilon)^2$ and $(F(R) \times h\upsilon)^{1/2}$ vs. $h\upsilon$ (eV).

2.4. Photocatalytic experiments

To examine the visible light photocatalytic performance of Ag_3PO_4/TiO_2 in terms of 2-CP degradation; Luzchem photochemical reactor (LZC4) system was used. In a typical experiment, fixed amount (varying from 0.5 to 1.5 $g{\cdot}L^{-1}$) of the photocatalyst was added in the 2-CP solution in a cylindrical quartz rector cell (250 mL capacity) provided with air circulation and magnetic stirring was provided to ensure thorough mixing. The reaction contents were irradiated with visible light lamps from top and sides with spectral range from 400 to 700 nm and spectral irradiance of 17.45 $mW{\cdot}m^{-2}$ monitored by Luzchem power monitor at a distance of 12 cm from the light source for a duration of 180 min irradiation time. For analysis 2.5 mL samples were drawn after every 30 min and analyzed by using UV–visible spectrophotometer (HACH LANGE DR6000) at λ = 274 nm. The 2-CP degradation efficiency was calculated, after analysis, using the following relation:

$$\text{Degradation } \% = \left\{\frac{\left(C_o C_t\right)}{C_o}\right\} \times 100 \quad (1)$$

where C_o and C_t denote initial and residual concentration of 2-CP ($mg{\cdot}L^{-1}$), respectively, and t is the irradiation time (min).

3. Results and discussion

3.1. Morphology, structural and optical properties of Ag_3PO_4/TiO_2

The X-ray diffraction (XRD) peaks corresponding to the body-centered cubic (bcc) phase of Ag_3PO_4 are presented in Fig. 1 for Ag_3PO_4/TiO_2 composite. The diffraction peaks for Ag_3PO_4 nanoparticles are represented in black font color at 2θ values 21.8°, 29.6°, 33.5°, 36.7°, 48.2°, 55.0°, 57.5°, 60.9° and

72.1° corresponding to the diffractions from the (110), (200), (210), (211), (310), (222), (320), (321) and (332) crystal planes. Results shown exhibit crystalline integrity as reported by Zhang et al. [23]and Wang et al. [28] and the XRD peaks for Degussa P25 are easily distinguishable from the XRD patterns with representative (101), (004), (200), (211) and (002) crystalline planes represented in red font color.

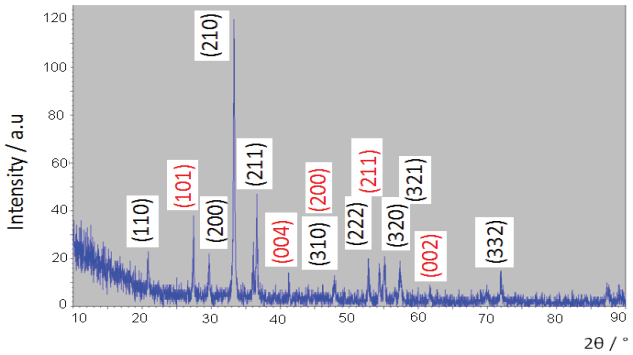

Fig. 1. XRD patterns of the prepared Ag_3PO_4/TiO_2 (molar ratio = 3:10) powder; Ag_3PO_4 (black font) and Degussa P25 (red font).

The porosity and surface area of the photocatalyst were analyzed by nitrogen physisorption using Quantachrome Autosorb IQ. After degassing the sample at a temperature of 200°C for 180 min, nitrogen porosimetry was performed at a temperature of 77 K over the 0 to 1 pressure ratio. Table 1 shows that TiO_2 exhibited a much higher surface area of 50 $m^2\ g^{-1}$ with a relatively higher pore volume of 0.1 $cm^3\ g^{-1}$compared with lower pore volume of 0.002 $cm^3\ g^{-1}$ and surface area of 1.6 $m^2\ g^{-1}$ of Ag_3PO_4 particles which provides suitable dispersion of Ag_3PO_4 within TiO_2 particles. The decline in surface area for Ag_3PO_4/TiO_2 nanocomposite to 15 $m^2\ g^{-1}$ could be attributed to smaller size of Ag_3PO_4 that can clog the pores of TiO_2 [29].

The FESEM and TEM images of synthesized Ag_3PO_4/TiO_2 nanoparticles are shown in Figs. 2(a) and (b), respectively, while Fig. 2(c) represents the TEM image of TiO_2. From the

Table 1
Porosimetric determinations of Ag_3PO_4/TiO_2

Catalyst	BET SSA ($m^2\ g^{-1}$)	Pore volume ($cm^3\ g^{-1}$)
Degussa P25	50	0.1
Ag_3PO_4/TiO_2	15	0.0358
Ag_3PO_4	1.6	0.002

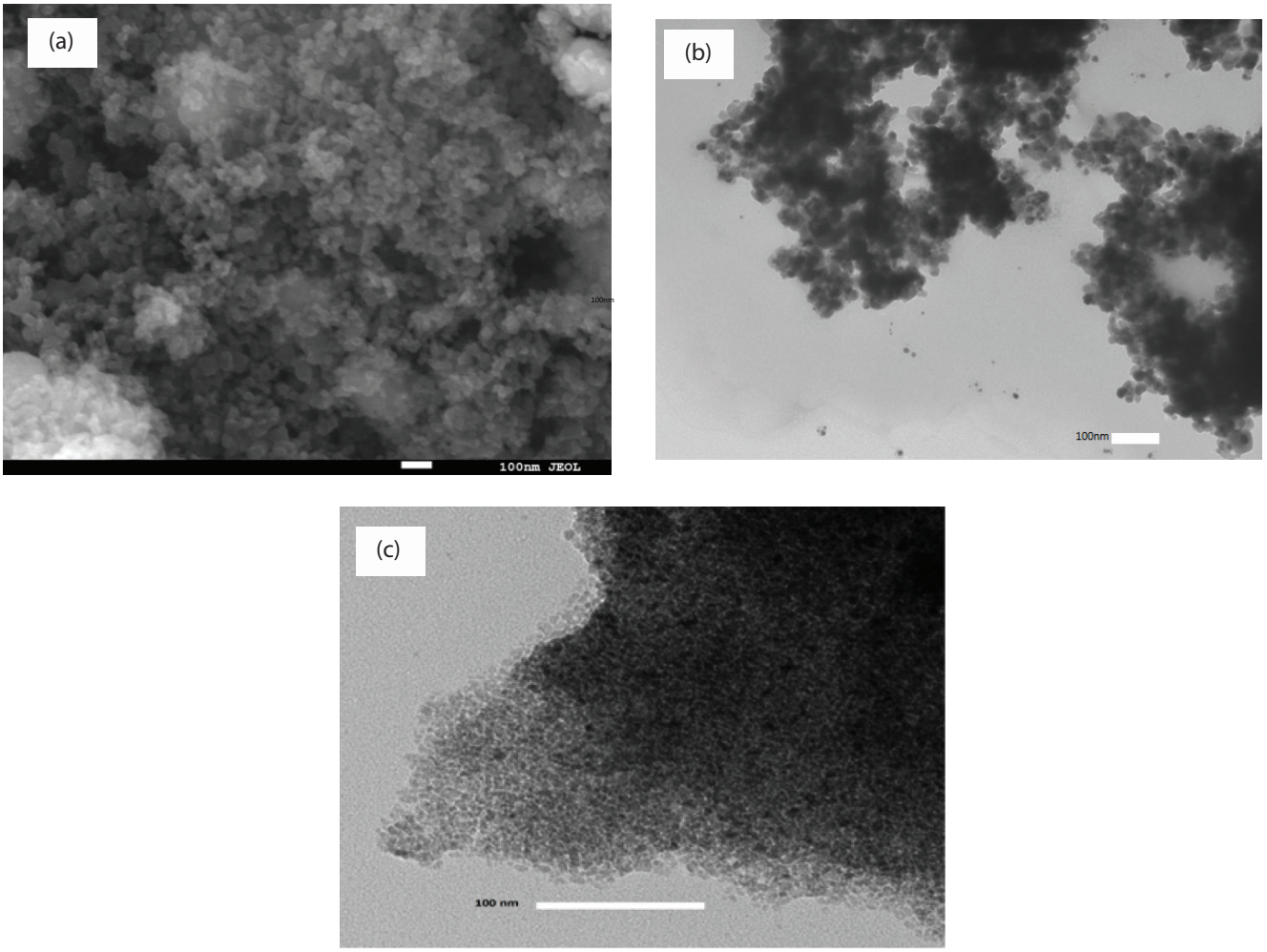

Fig. 2. (a) FESEM and (b) TEM images of Ag_3PO_4/TiO_2 and (c) TEM image of TiO_2.

TEM image of the composite Ag_3PO_4/TiO_2 photocatalyst, two distinct particles are identified. The TiO_2 particles fairly appear in nanometer scale while with average particles size of 20–30 nm diameters represent while the finer particles mainly deposited on the surface of TiO_2 in the Ag_3PO_4/TiO_2 nanocomposite belong to Ag_3PO_4. The smaller size of Ag_3PO_4 nanoparticles can be attributed to the adsorption of silver ions onto the negatively charged surface of TiO_2 thus limiting the growth of Ag_3PO_4 particles concurrent with the Brunauer–Emmett–Teller (BET) surface area determinations [29].

The XPS survey analysis of the Ag_3PO_4/TiO_2 shown in Fig. 3(a) confirms the presence of Ag, P, Ti and O as sample constituents. Fig. 3(b) shows the high resolution XPS spectrum of Ag 3d characterized by two peaks with binding energy values of 367.55 and 373.65 corresponding to the Ag $3d_{5/2}$ and $3d_{3/2}$, respectively. Deconvolution of Ag 3d peaks resulted high intensity peaks at 367.72 and 373.73 eV representing Ag^+ and two low intensity peaks at 368.26 and 374.26 eV representing metallic silver Ag^o in the Ag_3PO_4/TiO_2 as reported by other studies [23,28,30]. The high resolution XPS spectrum of Ti 2p with $2p_{3/2}$ peaks at 458.69 and 459.29 eV suggests the presence of TiO_2 (Fig. 3(c)). The O 1s peak was observed at 530 eV with a shoulder toward high binding energy value as shown in Fig. 3(d). On deconvolution three component peaks with different intensities were identified. The highest intensity peak with binding energy value of 529.78 eV belongs to the anionic O_2^- from Ag_3PO_4 and TiO_2 [31]. The shoulder peaks include peaks with 531.04 and 532.43 eV identified as bound oxygen with Ag_2O and oxygen from adsorbed H_2O on the surface of TiO_2 [32]. Similarly, the peak at 133.15 eV (Fig. 3(e)) represents the P 2p core level peak characteristic of $(PO_4)^{3-}$ group [33]. The XPS results suggest that in situ deposition of $(PO_4)^{3-}$ and Ag^+ ions on the surface of TiO_2 yielded stable precipitated Ag_3PO_4/TiO_2 composites. XPS binding energies of Ag 3d, Ti 2p, O 1s, C 2p and P 2p along with the atomic % determined by quantitative XPS analysis of Ag_3PO_4/TiO_2 nanocomposite are provided in Table S1.

The solid state absorption and diffuse reflectance spectra of the Ag_3PO_4/TiO_2 showed two strong absorption edges around 420 and 520 nm corresponding to the absorption edges reported for TiO_2 (P25) and Ag_3PO_4, respectively [34]. Kubelka–Munk transformation was applied to the UV reflectance data of the synthesized nanoparticles to calculate the values of $F(R)$. The direct and indirect energy band gap of the synthesized Ag_3PO_4/TiO_2 nanoparticles was calculated by plotting $(F(R) \times h\upsilon)^2$ and $(F(R) \times h\upsilon)^{1/2}$ vs. $h\upsilon$, respectively. The indirect energy band gap of TiO_2 Degussa P25 and Ag_3PO_4/TiO_2 is shown in Fig. 4. From the plot the band gap energy (E_g) was determined by extrapolating the linear region of the plot on x-axis. Compared with the energy band gap of ~3.18 eV for Degussa P25 the direct energy band gap of the synthesized nanoparticles was found to be at ~2.52 eV while the indirect band gap was found to be ~2.3 eV which is consistent with the values reported by Huang et al. [35] for Ag_3PO_4. These results suggest that Ag_3PO_4/TiO_2 is an indirect band gap semiconductor.

4. Photocatalysis

Photocatalytic degradation is a light dependent process where the photocatalyst material utilizes the energy of incident photons equal to or greater than its energy band gap. The valence band (VB) electrons upon absorption of such photon energy are excited to the conduction band (CB) and leave behind a positively charged hole. The electron hole pair (e^-/h^+) thus formed is responsible for generation of reactive oxidizing species (e.g., $OH^\bullet$ and O_2^- radicals) through a series of oxidation reduction reactions in aqueous medium [36] and eventually breakdown the organic pollutants adsorbed on the catalyst surface. In case of Ag_3PO_4/TiO_2, upon exposure to visible light irradiation, the electrons in CB of Ag_3PO_4 may move to the surface of reduced TiO_2 that acts as a photoinduced electrons acceptor. This charge transfer from Ag_3PO_4 may result in unavailability of electrons to remaining Ag_3PO_4 particles that may result in increased photostability [29]. The absorbed oxygen on TiO_2 surface, however, may react with electrons forming reactive oxygen species such as aforementioned superoxides ($O_2^{\bullet-}$) which may further degrade the 2-CP molecules. Moreover, photoinduced holes in the VB of Ag_3PO_4 transfer to the VB of TiO_2 and can directly oxidize 2-CP molecules thus enhancing photocatalysis. Compared with Ag_3PO_4 and TiO_2 Degussa P25 the Ag_3PO_4/TiO_2 nanocomposite showed significant increase in the photocatalytic activity validating the importance of Ag_3PO_4 doping over TiO_2 surface (Fig. S1) for the visible light initiated photocatalysis.

$$Ag_3PO_4 + h\upsilon\left(E \geq E_g\right) \rightarrow e_{CB}^- + h_{VB}^+ \quad (2)$$

$$H_2O + h^+ \rightarrow H_2O^+ \rightarrow HO^\circ + H^+ \quad (3)$$

$$TiO_2\left(e_{VB}^- + O_2\right)ads + e^- \rightarrow O_2^- \quad (4)$$

$$H_2O \rightarrow HO^- + H^+ \quad (5)$$

$$HO^- + h^+ \rightarrow HO^\circ \quad (6)$$

$$O_2^- + H^- \rightarrow HOO^\circ \quad (7)$$

$$2HO^\circ \rightarrow H_2O_2 + \frac{1}{2}\left[O_2\right] \quad (8)$$

$$H_2O_2 + H^+ + e^- \rightarrow OH^\circ + H_2O \quad (9)$$

$$2\text{-CP} + OH^\circ \rightarrow \text{Intermediates} \rightarrow CO_2 + H_2O + HCl \quad (10)$$

Solution pH is one of the main controlling factors that determine the photocatalytic degradation process. The solution pH values lesser than point of zero charge of the photocatalyst material has been reported to facilitate hydroxyl radical and H_2O_2 formation [37]. Fig. 5 shows the effect of solution pH on the Ag_3PO_4/TiO_2 catalyzed degradation of 2-CP. For 50 mg·L^{-1} of initial 2-CP concentration and visible light irradiation for 180 min variation in solution pH values showed significant change in 2-CP degradation %. With the

change in solution pH from 3 to 5 and 7; the corresponding values of 2-CP degradation varied from 70% to 55.68% and 53.5%, respectively. At pH values higher than 6 TiO_2 surface bears negative charge and existence of electrostatic repulsion between aqueous phenolate ions and TiO_2 may be responsible for lower adsorption rates and corresponding degradation efficiency. Higher pH values have also been reported to decrease the degradation rates due to OH^- ions scavenging by thus formed carbonate ions [38]. The electrostatic binding of 2-CP at pH 3 facilitates adsorption of the pollutant onto the positively charged surface of Ag_3PO_4/TiO_2 that resulted in maximum degradation efficiency.

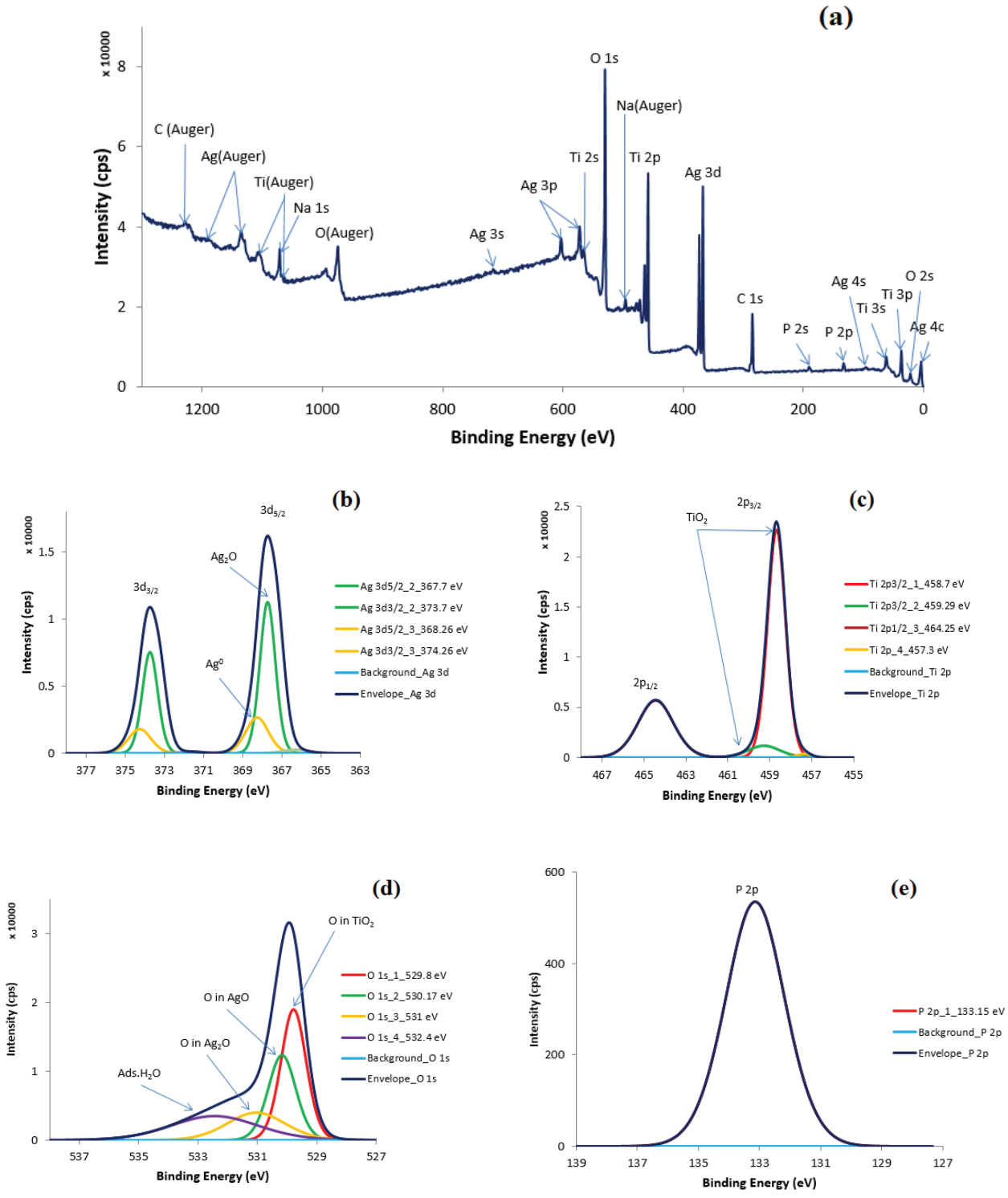

Fig. 3. (a) XPS scan of Ag_3PO_4/TiO_2; (b)–(e) XPS spectra of Ag 3d, Ti 2p, O 1s and P 2p.

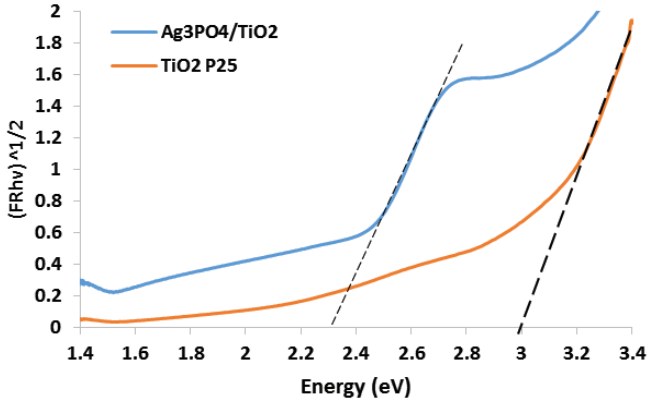

Fig. 4. Calculation of indirect energy band gap of Ag_3PO_4/TiO_2 and Degussa P25.

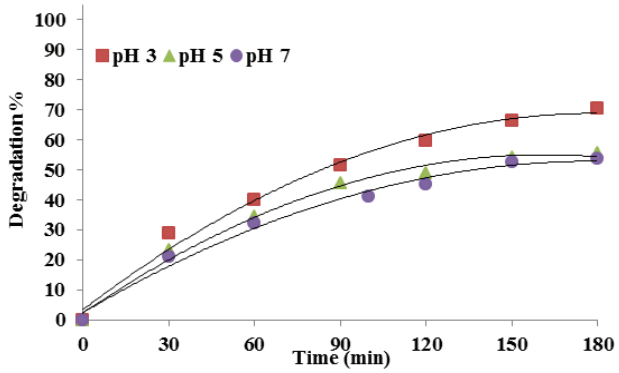

Fig. 5. Effect of pH change on photocatalytic degradation of 2-CP (catalyst dose = 1 g·L^{-1}, 2CP concentration = 50 mg·L^{-1}, visible irradiation = 112 W).

In a separate series of experiments 0.5–1.5 g·L^{-1} of Ag_3PO_4/TiO_2 was added to 50 mg·L^{-1} 2-CP solution to evaluate the catalyst dose effect on photocatalytic degradation. As shown in Fig. 6, an initial increase in catalyst dose from 0.5 to 1 g·L^{-1} showed increase in degradation efficiency from 56% to 70.3% attributed to increased number of catalyst active sites with catalyst dose. However, further increase in catalyst dose to 1.5 g·L^{-1} showed decrease in degradation efficiency up to 41.4%. At high catalyst dose catalyst agglomeration becomes significant, thus reducing the overall surface area and subsequently the availability of catalyst active sites for reaction [39]. Also at higher catalyst dose decline in penetration of light and increased outward scattering becomes more significant thus manifesting in lowered photocatalytic degradation rate [39].

The photocatalytic performance of Ag_3PO_4/TiO_2 under optimized conditions was investigated over a wide initial pollutant concentration range from 15 to 50 mg·L^{-1} (Fig. 7). Keeping the catalyst dose of 1 g·L^{-1}, 100% degradation efficiency was observed when 15 mg·L^{-1} of 2-CP was exposed to visible light for 120 min. However, further increase in 2-CP concentration to 25 and 50 mg·L^{-1} resulted in decrease in degradation efficiency from 92.5% to 70.3%, respectively, for 180 min of irradiation time. This can be attributed to the decreased probability of 2-CP molecules to react with the

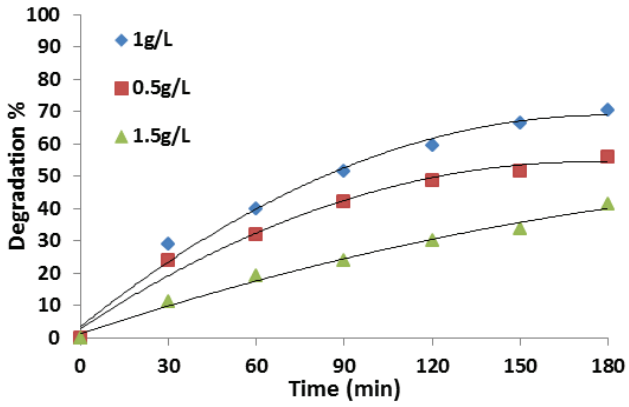

Fig. 6. Effect of catalyst dose on photocatalytic degradation of 2-CP (pH = 3, 2CP concentration = 50 mg·L^{-1}, visible irradiation = 112 W).

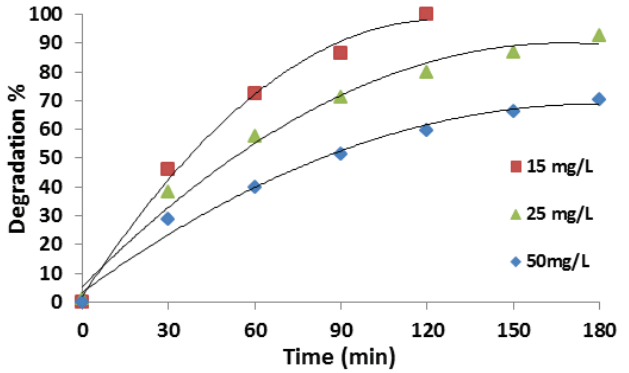

Fig. 7. Effect of catalyst dose on photocatalytic degradation of 2-CP (pH = 3, catalyst dose = 1 g·L^{-1}, visible irradiation = 112 W).

active species on the surface of Ag_3PO_4/TiO_2 with increase in initial pollutant concentration.

In order to evaluate the structural stability of the photocatalyst, Ag_3PO_4/TiO_2 was recovered after use from the solution by decanting and centrifugation followed by washing with distilled water, filtration and drying at 40°C for 180 min. The recovered catalyst was subjected to reuse for three times with fresh 2-CP solution whereby it retained stability and showed 100% visible light degradation efficiency for 15 mg·L^{-1} of 2-CP as shown in Fig. 8(a) while the recyclability of pristine Ag_3PO_4 is provided in Fig. 8(b). The movement of photoexcited electrons from Ag_3PO_4 to TiO_2 nanoparticles results in reduction in metallic Ag^o formation that is apparent as stabilization of the Ag_3PO_4/TiO_2 nanocomposite and higher recyclability of the photocatalyst as demonstrated by similar studies [40].

The rate of reaction at very low pollutant concentration (mg·L^{-1} level) is dependent on the initial pollutant concentration as evidenced by similar studies [41,42]. The variation in the rate of photocatalytic degradation of 2-CP with experimental parameters was evaluated by fitting the experimental data with the pseudo-first-order reaction kinetic model. Eq. (11) represents the simplified version of the generally adopted model for degradation of organic pollutants in solution [43].

$$\ln\left(\frac{C_o}{C}\right) = k_{app}t \quad (11)$$

The apparent rate constant k_{app} was calculated from the plot of $(\ln(C_o/C))$ vs. irradiation time t as shown in Fig. 9. The values of rate constant decreased from 0.0231 to 0.006 min^{-1} with increase in initial 2-CP concentration from 15 to 50 $mg{\cdot}L^{-1}$ which is interpreted as the decrease in photocatalytic efficiency. Increasing the number of 2-CP molecules per unit volume resulted lower light penetration to the surface of the photocatalyst particles thus slowing the rate of photocatalytic degradation. The observed values of kinetic parameters as a function of 2-CP initial concentration, pH and catalyst dose are provided in Table 2.

5. Conclusions

In situ precipitation method was adopted to synthesize stable visible light active Ag_3PO_4/TiO_2 nanoparticles photocatalyst. The photocatalytic activity of the synthesized catalyst was successfully tested for degradation of 2-CP under

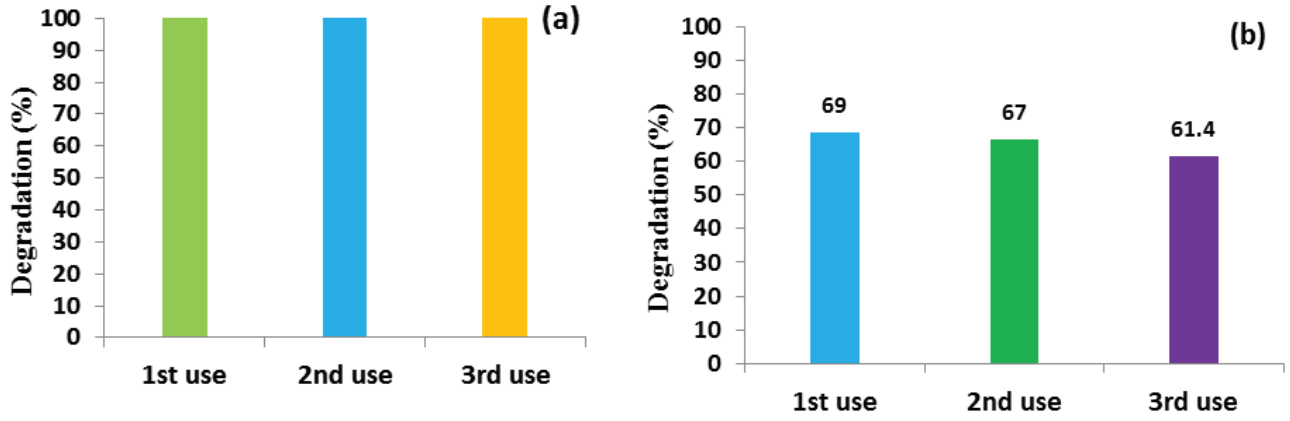

Fig. 8. Catalyst reuse (a) $Ag_3PO_4TiO_2$ and (b) Ag_3PO_4 (catalyst dose = 1g·L⁻¹, pH = 3, 2-CP concentration = 15 mg·L⁻¹, visible irradiation = 112 W).

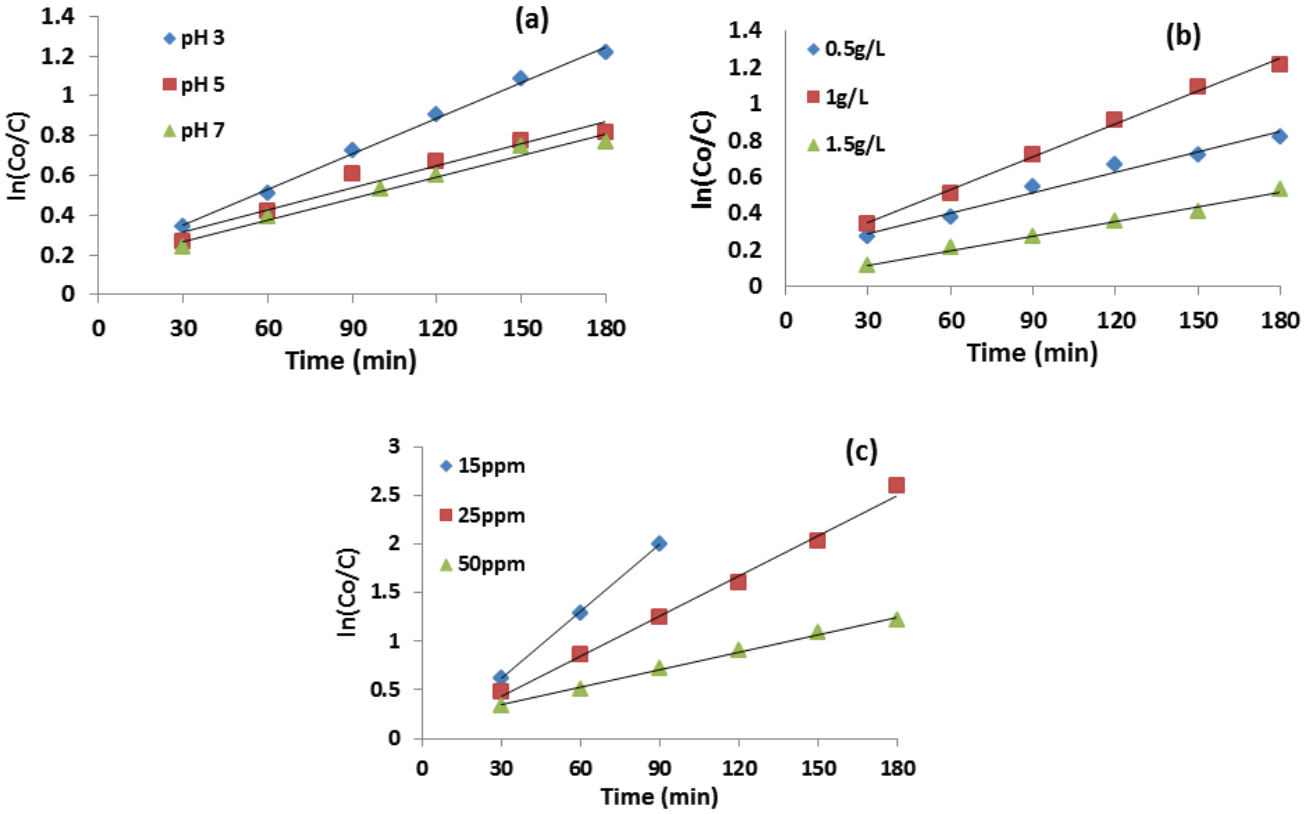

Fig. 9. Pseudo-first-order kinetic plots for degradation of 2-CP by Ag_3PO_4/TiO_2 under variable (a) solution pH, (b) catalyst dose and (c) pollutant concentration.

Table 2
Effects of catalyst dose, solution pH and initial 2-CP concentration on the photocatalytic activity of Ag_3PO_4/TiO_2

Catalyst dose ($g·L^{-1}$)[a]	k_{app} (min^{-1})	R^2	Solution pH[b]	k_{app} (min^{-1})	R^2	Initial 2-CP concentration ($mg·L^{-1}$)[c]	k_{app} (min^{-1})	R^2
0.5	0.0037	0.98	3	0.006	0.9956	15	0.0231	0.9998
1	0.006	0.9956	5	0.0037	0.9496	25	0.0137	0.9926
1.5	0.0026	0.9896	7	0.0036	0.9767	50	0.006	0.9956

[a]2-CP = 50 $mg·L^{-1}$, pH = 3, time = 180 min, visible light lamp = 112 W.
[b]2-CP = 50 $mg·L^{-1}$, catalyst dose = 1 $g·L^{-1}$, time = 180 min, visible light lamp = 112 W.
[c]Catalyst dose = 1 $g·L^{-1}$, time = 180 min, pH = 3, visible light lamp = 112 W.

visible irradiation. The XRD and TEM studies suggested that the nanocrystals obtained were polycrystalline with average particle size for Degussa P25 in the range of 28–78 nm while 10–17 nm for Ag_3PO_4. The XPS analysis results confirmed the presence of Ag, P, O and Ti elements with their respective oxidation states corresponding to Ag_3PO_4/TiO_2. The synthesized photocatalysts showed high photoactivity with complete degradation of 15 $mg·L^{-1}$ 2-CP achieved at pH 3 within 120 min and 92.5% degradation of 25 $mg·L^{-1}$ within 180 min of visible light irradiation. The kinetic interpretation of experimental results suggests that the photodegradation of 2-CP closely followed the pseudo-first-order reaction kinetics with maximum k_{app} value of 0.0231 min^{-1}.

Acknowledgments

The authors gratefully acknowledge King Abdulaziz University (KAU, Saudi Arabia) for funding this work (grant # 001 MET 01 USA 01), and University of South Florida (USF, USA).

References

[1] M.A. Henderson, A surface science perspective on TiO_2 photocatalysis, Surf. Sci. Rep., 66 (2011) 185–297.
[2] A. Fujishima, X. Zhang, D.A. Tryk, TiO_2 photocatalysis and related surface phenomena, Surf. Sci. Rep., 63 (2008) 515–582.
[3] A. Fujishima, K. Honda, Electrochemical photolysis of water at a semiconductor electrode, Nature, 238 (1972) 37–38.
[4] E. Kowalska, H. Remita, C. Colbeau-Justin, J. Hupka, J. Belloni, Modification of titanium dioxide with platinum ions and clusters: application in photocatalysis, J. Phys. Chem. C, 112 (2008) 1124–1131.
[5] M.H. Hernández-Alonso, F. Fresno, S. Suárez, J.M. Coronado, Development of alternative photocatalysts to TiO_2: challenges and opportunities, Energy Environ. Sci., 2 (2009) 1231–1257.
[6] M.A. Lazar, S. Varghese, S.S. Nair, Photocatalytic water treatment by titanium dioxide: recent updates, Catalysts, 2 (2012) 572–601.
[7] M.N. Chong, B. Jin, C.W.K. Chow, C. Saint, Recent developments in photocatalytic water treatment technology: a review, Water Res., 44 (2010) 2997–3027.
[8] A. Fujishima, T.N. Rao, D.A. Tryk, Titanium dioxide photocatalysis, J. Photochem. Photobiol. C, 1 (2000) 1–21.
[9] S. Rehman, R. Ullah, A.M. Butt, N.D. Gohar, Strategies of making TiO_2 and ZnO visible light active, J. Hazard. Mater., 170 (2009) 560–569.
[10] F.R. Xiu, F.S. Zhang, Preparation of nano-Cu_2O/TiO_2 photocatalyst from waste printed circuit boards by electrokinetic process, J. Hazard. Mater., 172 (2009) 1458–1463.
[11] Y. Kondo, H. Yoshikawa, K. Awaga, M. Murayama, T. Mori, K. Sunada, S. Bandow, S. Iijima, Preparation, photocatalytic activities, and dye-sensitized solar-cell performance of submicron-scale TiO_2 hollow spheres, Langmuir, 24 (2008) 547–550.
[12] T.J. Whang, H.Y. Huang, M.T. Hsieh, J.J. Chen, Laser-induced silver nanoparticles on titanium oxide for photocatalytic degradation of methylene blue, Int. J. Mol. Sci., 10 (2009) 4707–4718.
[13] S.H.S. Chan, T.Y. Wu, J.C. Juan, C.Y. Teh, Recent developments of metal oxide semiconductors as photocatalysts in advanced oxidation processes (AOPs) for treatment of dye waste-water, J. Chem. Technol. Biotechnol., 86 (2011) 1130–1158.
[14] W.J. Zhou, H. Liu, J.Y. Wang, D. Liu, G.J. Du, J.J. Cui, Ag_2O/TiO_2 nanobelts heterostructure with enhanced ultraviolet and visible photocatalytic activity, ACS Appl. Mater. Interfaces, 2 (2010) 2385–2392.
[15] C.C. Chen, X.Z. Li, W.H. Ma, J.C. Zhao, H. Hidaka, N. Serpone, Effect of transition metal ions on the TiO_2-assisted photodegradation of dyes under visible irradiation: a probe for the interfacial electron transfer process and reaction mechanism, J. Phys. Chem. B, 106 (2002) 318–324.
[16] X. Yang, H. Tang, J. Xu, M. Antonietti, M. Shalom, Silver phosphate/graphitic carbon nitride as an efficient photocatalytic tandem system for oxygen evolution, Chem. Sustain. Chem., 8 (2015) 1350–1358.
[17] X. Yang, J. Qin, Y. Jiang, K. Chen, X. Yan, D Zhang, R. Li, H. Tang, Fabrication of $P25/Ag_3PO_4$/graphene oxide heterostructures for enhanced solar photocatalytic degradation of organic pollutants and bacteria, Appl. Catal., B, 166 (2015) 231–240.
[18] H. Katsumata, M. Taniguchi, S. Kaneco, T. Suzuki, Photocatalytic degradation of bisphenol A by Ag_3PO_4 under visible light, Catal. Commun., 34 (2013) 30–34.
[19] Z.M. Yang, Y. Tian, G.-F. Huang, W.Q. Huang, Y.Y. Liu, C. Jiao, Z. Wan, X.G. Yan, A. Pan, Novel 3D flower-like Ag_3PO_4 microspheres with highly enhanced visible light photocatalytic activity, Mater. Lett., 116 (2014) 209–211.
[20] X.G. Ma, B. Lu, D. Li, R. Shi, C.S. Pan, Y.F. Zhu, Origin of photocatalytic activation of silver orthophosphate from first principles, J. Phys. Chem., C, 115 (2011) 4680–4687.
[21] X. Yang, J. Qin, Y. Jiang, R. Li, Y. Li, H. Tang, Bifunctional TiO_2/Ag_3PO_4/graphene composites with superior visible light photocatalytic performance and synergistic inactivation of bacteria, RSC Adv., 4 (2014) 18627–18636.
[22] X. Yang, Z. Chen, J. Xu, H. Tang, K. Chen, Y. Jiang, Tuning the morphology of g-C_3N_4 for improvement of Z-scheme photocatalytic water oxidation, ACS Appl. Mater. Interfaces, 7 (2015) 15285–15293.
[23] S. Zhang, X. Gu, Y. Zhao, Y. Qiang, Effect of annealing temperature and time on structure, morphology and visible-light photocatalytic activities Ag_3PO_4 microparticles, Mater. Sci. Eng., B, 201 (2015) 57–65.
[24] S.H. Lin, C.H. Chiou, C.K. Chang, R.S. Juang, Photocatalytic degradation of phenol on different phases of TiO_2 particles in aqueous suspensions under UV irradiation, J. Environ. Manage., 92 (2011) 3098–3104.
[25] EPA, Code of Federal Regulations, Appendix A to Part 423, 126 Priority Pollutants, 2014. Available at: http://www.epa.gov/sites/production/files/2015-09/documents/priority-pollutant-list-epa.pdf
[26] Directive on Environmental Quality Standards (Directive 2008/105/EC). Available at: http://eur-lex.europa.eu/LexUriServ/LexUriServ.do?uri=OJ:L:2008:348:0084:0097:en:PDF

[27] J. Xu, F. Wang, W. Liu, W. Cao, Nanocrystalline N-doped TiO_2 powders: mild hydrothermal synthesis and photocatalytic degradation of phenol under visible light irradiation, Int. J. Photoenergy, 2013 (2013) 1–7.
[28] D. Wang, Z. Li, L. Shang, J. Liu, J. Shen, Heterostructured Ag_3PO_4/TiO_2 film with high efficiency for degradation of methyl orange under visible light, Thin Solid Films, 551 (2014) 8–12.
[29] X. Cui, Y. Li, Q. Zhang, H. Wang, Silver orthophosphate immobilized on flaky layered double hydroxides as the visible-light-driven photocatalysts, Int. J. Photoenergy, 2012 (2012) 1–6.
[30] H. Zhang, G. Wang, D. Chen, X. Lv, J. Li, Tuning Photoelectrochemical Performances of Ag–TiO_2 nanocomposites via reduction/oxidation of Ag, Chem. Mater., 20 (2008) 6543–6549.
[31] M. Ge, N. Zhu, Y.P. Zhao, J. Li, L. Liu, Sunlight-assisted degradation of dye pollutants in Ag_3PO_4 suspension, Ind. Eng. Chem. Res., 51 (2012) 5167–5173.
[32] J.G. Yu, J.F. Xiong, B. Cheng, S.W. Liu, Fabrication and characterization of Ag–TiO_2 multiphase nanocomposite thin films with enhanced photocatalytic activity, Appl. Catal., B, 60 (2005) 211–221.
[33] M. Pelavin, D. Hendrickson, J. Hollander, W. Jolly, Phosphorus 2p electron binding energies. Correlation with extended Hueckel charges, J. Phys. Chem., 74 (1970) 1116–1121.
[34] X. Ma, H. Li, Y. Wang, H. Li, B. Liu, S. Yin, T. Sato, Substantial change in phenomenon of self-corrosion on Ag_3PO_4/TiO_2 compound photocatalyst, Appl. Catal., B, 158–159 (2014) 314–320.
[35] G.F. Huang, Z.L. Ma, W.Q. Huang, Y. Tian, C. Jiao, Z.M. Yang, Z. Wan, A. Pan, Ag_3PO_4 semiconductor photocatalyst: possibilities and challenges, J. Nanomater., 2013 (2013) 1–8.
[36] U.I. Gaya, A.H. Abdullah, Heterogeneous photocatalytic degradation of organic contaminants over titanium dioxide: a review of fundamentals, progress and problems, J. Photochem. Photobiol., C, 9 (2008) 1–12.
[37] P. Pichat, Photocatalysis and Water Purification from Fundamentals to Recent Applications, 1st ed., Wiley-VCH Verlag, GmBH Germany, 2013.
[38] K. Naeem, O. Feng, Parameters effect on heterogeneous photocatalyzed degradation of phenol in aqueous dispersion of TiO_2, J. Environ. Sci., 21 (2009) 527–533.
[39] J.C. Sin, S.M. Lam, A.R. Mohamed, K.T. Lee, Degrading endocrine disrupting chemicals from wastewater by TiO_2 photocatalysis: a review, Int. J. Photoenergy, 2012 (2012) 1–23.
[40] X. Yang, H. Cui, Y. Li, J. Qin, R. Zhang, H. Tang, Fabrication of Ag_3PO_4-graphene composites with highly efficient and stable visible light photocatalytic performance, ACS Catal., 3 (2013) 363–369.
[41] G. Zhang, J. Gong, X. Zou, F. He, H. Zhang, Q. Zhang, Y. Liu, X. Yang, B. Hu, Photocatalytic degradation of azo dye acid red G by KNb_3O_8 and the role of potassium in the photocatalysis, Chem. Eng. J., 123 (2006) 59–64.
[42] I. Bouzaida, C. Ferronato, J.M. Chovelon, M.E. Rammah, J.M. Herrmann, Heterogeneous photocatalytic degradation of the anthraquinonic dye, Acid Blue 25 (AB25): a kinetic approach, J. Photochem. Photobiol., A, 168 (2004) 23–30.
[43] S. Buzby, M.A. Barakat, H. Lin, C. Ni, S.A. Rykov, J.G. Chen, S. Ismat Shah, Visible light photocatalysis with nitrogen-doped titanium dioxide nanoparticles prepared by plasma assisted chemical vapor deposition, J. Vac. Sci. Technol., B, 24 (2006) 1210–1214.

Supplementary data

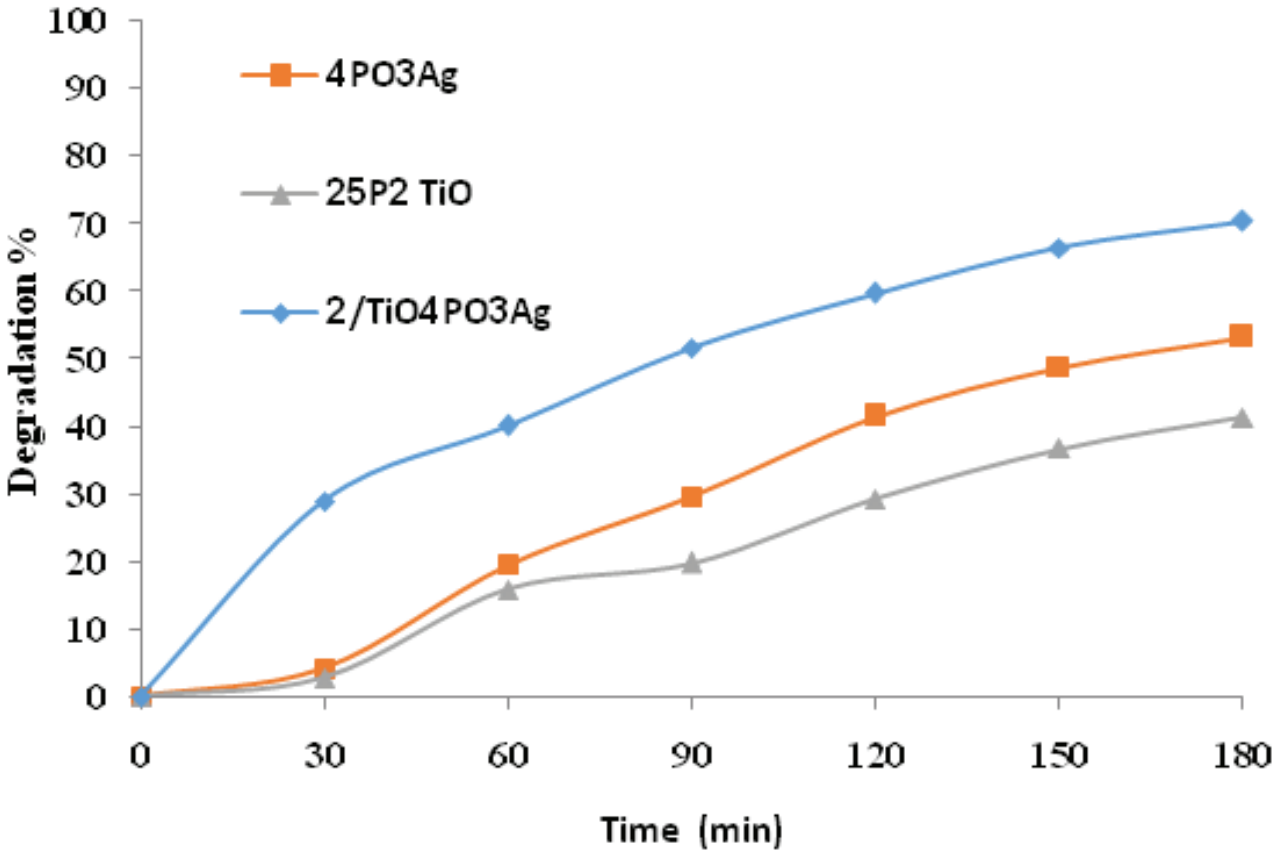

Fig. S1. Comparison of photocatalytic activities for degradation of 2-CP (solution pH = 3, catalyst dose = 1 g·L[1], Vis. Irradiation = 112 W, pollutant concentration = 50 mg·L^{-1}).

Table S1
XPS binding energies of Ag 3d, Ti 2p, O 1s, C 2p and P 2p determined by quantitative XPS analysis for Ag_3PO_4/TiO_2 nanocomposite

Elements	Binding energy position (eV)						Atomic %
	Peak 1	Peak 2	Peak 3	Peak 4	Peak 5	Peak 6	
Ag 3d	367.1	367.7	368.26	373.1	373.7	374.26	5.482
Ti 2p	458.7	459.7	464.25				12.384
O 1s	529.8	530.17	531	532.4			49.181
C 1s	284.95	286.67	288.92				28.464
P 2p	131.15						2.521